Original Article

Influence of cardiac cycle on myocardial extracellular volume fraction measurements with dual-layer computed tomography

Daisuke Nishigake[1], Yuzo Yamasaki[2], Tomoyuki Hida[2], Takashi Shirasaka[1], Ryohei Funatsu[1], Toyoyuki Kato[1], Kousei Ishigami[2]

[1]Division of Radiology, Department of Medical Technology, Kyushu University Hospital, Fukuoka, Japan; [2]Department of Clinical Radiology, Graduate School of Medical Sciences, Kyushu University, Fukuoka, Japan

Contributions: (I) Conception and design: All authors; (II) Administrative support: D Nishigake, Y Yamasaki, T Hida; (III) Provision of study materials or patients: Y Yamasaki, T Hida, K Ishigami; (IV) Collection and assembly of data: D Nishigake, Y Yamasaki, T Hida; (V) Data analysis and interpretation: D Nishigake, Y Yamasaki, T Hida; (VI) Manuscript writing: All authors; (VII) Final approval of manuscript: All authors.

Correspondence to: Yuzo Yamasaki, MD, PhD. Department of Clinical Radiology, Graduate School of Medical Sciences, Kyushu University, 3-1-1, Maidashi, Higashi-ku, Fukuoka 812-8583, Japan. Email: yamasaki.yuzo.776@m.kyushu-u.ac.jp.

Background: In cardiac computed tomography (CT), the best image quality is obtained at mid-diastole at low heart rates (HRs) and at end-systole at high HRs. On the other hand, extracellular volume (ECV) measurements may be influenced by the cardiac phase. Therefore, we aimed to clarify the influence of the cardiac phase on the image quality and ECV values obtained using dual-layer spectral computed tomography (DLCT).

Methods: Fifty-five patients (68.0±14.5 years; 26 men) with cardiac diseases who underwent retrospective electrocardiogram-gated myocardial CT delayed enhancement (CTDE) between February 2019 to April 2022 were enrolled. The ECVs at the right ventricle (RV) and left ventricle (LV) walls in the end-systolic and mid-diastolic phases were calculated using iodine-density measurements from CTDE spectral data. Iodine-density image quality was classified on a 4-point scale. ECV and image quality across cardiac phases were compared using the t-test and Wilcoxon signed-rank test, respectively. Inter- and intraobserver variability were evaluated using intraclass correlation coefficient (ICC) values.

Results: The ECV of the septal regions during mid-diastole was significantly higher than that during end-systole. Other regions showed similar ECV measurements in both groups (P=0.13–0.97), except for the LV anterior wall and LV posterior wall at the base-ventricular level. The image-quality score in end-systole was significantly higher than that in mid-diastole (systole *vs.* diastole: 3.6±0.5 *vs.* 3.2±0.7; P=0.0195). Intra- and interobserver variabilities for RV ECV measurements at the end-systolic phase were superior to those at the mid-diastolic phase, whereas the corresponding values for LV ECV measurements were similar.

Conclusions: Septal ECV showed small but significant differences while other region ECV showed no difference during the cardiac cycle. RV ECV measurements in the end-systolic phase were more reproducible than those in the mid-diastolic phase.

Keywords: Extracellular volume (ECV); myocardial computed tomography delayed enhancement (myocardial CTDE); dual-layer computed tomography; cardiac cycle

Submitted Nov 20, 2023. Accepted for publication May 22, 2024. Published online Jun 18, 2024.
doi: 10.21037/qims-23-1647
View this article at: https://dx.doi.org/10.21037/qims-23-1647

Introduction

Extracellular volume (ECV) fraction measurements obtained using cardiac magnetic resonance T1 mapping have been validated as discriminators of myocardial disease (1-3) and used for risk stratification of cardiac events (4,5). Although cardiac magnetic resonance imaging (MRI) can be performed without radiation exposure, it may require longer acquisition times, yield limited imaging sections, and show limited applicability for patients who require mechanical device support. Gadolinium-enhanced cardiac MRI is also contraindicated in patients with severely impaired renal function, contrast allergy, and active asthma. It is difficult for patients who are critically ill to tolerate acquisitions involving multiple and long breath holds.

Cardiac computed tomography (CT) is widely used for coronary artery imaging owing to its high accessibility, low acquisition times, high spatial resolutions, and suitability for use in patients with mechanical devices and those undergoing dialysis. The introduction of dual-layer spectral CT (DLCT) has enabled ECV measurements using myocardial CT delayed enhancement (CTDE) imaging without non-contrast images. This system uses a detector-based dual-energy technique to measure the high- and low-energy projection data in the two detector layers simultaneously at the same spatial and angular locations, and can help prevent the misregistration associated with the subtraction-derived ECV method using pre- and post-contrast images. It can also facilitate the acquisition of clearer and finer images and may improve assessments of thinner and smaller structures, such as the right ventricle (RV), and patients with high heart rates (HRs). Therefore, this modality has evolved to yield myocardial characterizations comparable to ECV quantification using cardiac MRI (6-11).

The end-systolic or mid-diastolic phases are frequently used for assessment of cardiac structure because of the minimal motion in these phases. Yamasaki *et al.* recently demonstrated that DLCT with systolic-phase acquisition could reliably measure RV ECV and concluded that the CT-ECV measurements may be a surrogate marker of reverse tissue remodeling in chronic thromboembolic pulmonary hypertension, a form of pulmonary hypertension (12). On the other hand, Kidoh *et al.* reported a change of approximately 2% in the global left ventricle (LV) ECV during the cardiac cycle in a patient with hypertrophic cardiomyopathy, indicating the influence of the cardiac cycle on ECV values (13). This difference can also appear in structures other than the LV. One previous study also reported that the best image quality in cardiac CT was obtained at mid-diastole at low HRs and at end-systole at high HRs (14). Thus, ECV measurements may also be influenced by the cardiac phase. Thus, this study aimed to compare the image quality and ECV fraction of both ventricles in the diastolic and systolic phases and to clarify which phase is appropriate for ECV assessment using DLCT. We present this article in accordance with the STROBE reporting checklist (available at https://qims.amegroups.com/article/view/10.21037/qims-23-1647/rc).

Methods

Study population

The study was conducted in accordance with the Declaration of Helsinki (as revised in 2013). This retrospective observational study was approved by the Institutional Review Board of Kyushu University (No. 2023-72), and the requirement for informed consent was waived due to the retrospective nature of the study. Eighty-four consecutive patients who had or were suspected of having cardiac disease and underwent CTDE at our institution between February 2019 and April 2022 were screened. We excluded cases with (I) metal artifacts after cardiac surgery and (II) poor image quality that disables the identification of the myocardium. The patients were divided into 2 groups based on their HR (>70 and ≤70), and the effect of HR on the results was evaluated.

CT acquisition parameters

All patients underwent coronary CT, pulmonary angiography, transcatheter aortic valve implantation planning CT, or ablation planning CT, and CTDE (iQon Spectral CT, Philips Healthcare, Best, the Netherlands) using 80–100 mL of contrast medium [Iopamidol (Iopamiron 370; Bayer HealthCare, Osaka, Japan), Iohexol (Omuniparqu 300 or 350; GE HealthCare, Tokyo, Japan), or Ioversol (Optiray 320 or 350; Guerbet Japan, Tokyo, Japan)]. After 10 min, CTDE scans were obtained using retrospective electrocardiogram gating and the following parameters: detector collimation, 64×0.625 mm; tube rotation time, 270 ms; and tube voltage, 120 kVp; and scan mode, helical scan. The tube current was controlled using automatic exposure control (dose right index, 37).

Myocardial ECV measurement

Using spectral CTDE scan data, axial-source monochromatic

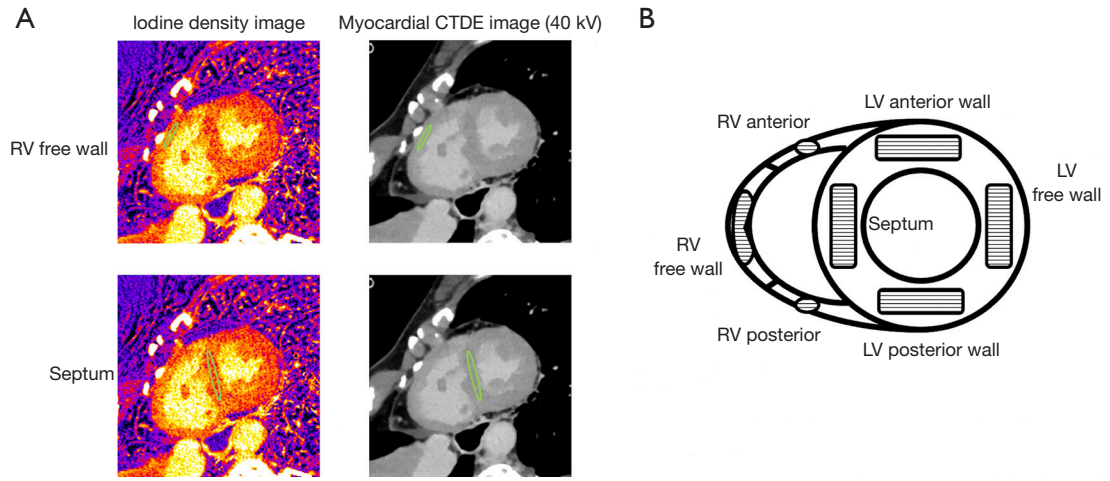

Figure 1 Color-coded iodine maps and myocardial CTDE images. (A) Iodine-density measurements in the right ventricular free wall (upper) and septum (lower). (B) Schematic of the region of interest placement for extracellular volume measurement. RV, right ventricle; CTDE, computed tomography delayed enhancement; LV, left ventricle.

40-kV images (CTDE images) and iodine-no-water images were reconstructed with section thicknesses and intervals of 0.8 and 0.4 mm, respectively, at cardiac phases of 40% (end-systole) and 80% (mid-diastole). Each original dataset of the axial images was processed for multiplanar reformation in the short-axis plane with a section thickness of 2.0 mm. The iodine density in each structure in the iodine-no-water images was measured by copying the regions of interest (ROIs) from the images at a workstation (IntelliSpace Portal version 10.1; Philips Healthcare, Best, the Netherlands) (*Figure 1*). We used 40-kV images, which had the highest contrast-to-noise ratio (15), for easy differentiation of the myocardium from the surrounding structures. The heart was divided into three sections in the long axis and four-chamber views: apex, mid, and base. ECV was measured in the slice at the center of the base and mid sections. The ROIs were drawn manually for the myocardium as large as possible from the epicardium to the endocardium avoiding the very edges of the myocardium so that partial volume averaging from the myocardial-blood interface. Each ROI was placed by a radiation technologist (D.N.) with 5 years of experience in cardiac CT and MRI. The iodine-density-derived CT-ECV was calculated as follows: CT-ECV (%) = (1 – hematocrit) × (iodine density in myocardium/iodine density in the LV blood pool) × 100 (12). The ECVs were measured at the LV anterior wall, septum, LV posterior wall, LV free wall, RV anterior wall, RV free wall, and RV posterior wall in the LV short-axis view of the mid- and base-ventricular levels at the end-systole and mid-diastole phases, respectively. The apex level was not measured to avoid partial-volume effects (9). Iodine-density image quality was subjectively classified on a 4-point scale by two cardiovascular radiologists (Y.Y. and T.H.) with 15 and 14 years of experience, respectively (4 = perfect image quality without artifacts, 3 = slightly impaired image quality, e.g., by mild grainy and speckled, 2 = severe impaired image quality, but not involving the whole segment, or 1 = severely impaired image quality involving the whole segment, but the myocardium can be identified, and the ROI can be placed).

Reproducibility

To determine the reproducibility of measurements for each imaging modality, image analysis of 20 randomly selected patients was repeated at least 1 month later by a radiation technologist (D.N.) and a cardiovascular radiologist (Y.Y.) who was blinded to the results of the initial study and clinical and experimental data.

Statistical analysis

JMP Pro 15.10 (SAS Institute, NC, USA) was used for statistical analysis. Statistical significance was set at $P<0.05$. The Shapiro-Wilk test was applied to test for normally distributed data. Normally distributed continuous variables are presented as mean± standard deviation. ECV measurements in the low- and high-HR groups were compared using the paired *t*-test. Patient characteristics of

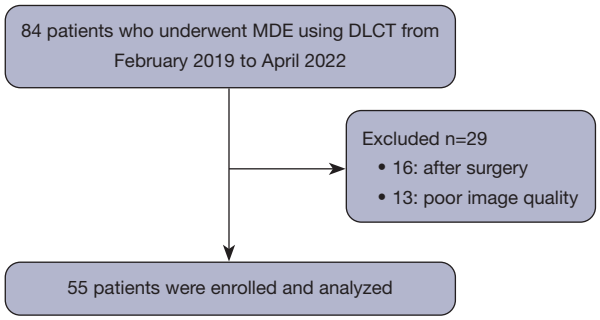

Figure 2 Patient flow diagram. MDE, myocardial delayed enhancement; DLCT, dual layer computed tomography.

Table 1 Baseline characteristics of the patients

Characteristic	Variable
Age (years)	68.0±14.5
Sex (male:female)	26:29
Heart rate (bpm)	72.7±18.4
Body mass index (kg/m^2)	23.9±3.9
Atrial fibrillation	16 (29.1)
Chronic thromboembolic pulmonary hypertension	13 (23.6)
Aortic valve stenosis	10 (18.2)
Pulmonary embolism	4 (7.3)
Coronary artery disease	2 (3.6)
Sarcoidosis	1 (1.8)
Chronic heart failure	1 (1.8)
Mitral regurgitation	1 (1.8)
Heart failure with preserved ejection fraction	1 (1.8)
Pulmonary arterial hypertension	1 (1.8)
Pulmonary hypertension associated with lung diseases and/or hypoxia	1 (1.8)
Patent ductus arteriosus	1 (1.8)
Pericarditis constrictive	1 (1.8)
Aortic valve regurgitation	1 (1.8)
Unknown	1 (1.8)

Values are expressed as mean ± standard deviation or n (%).

categorical variables between the low and high HR groups were compared using χ^2 test and continuous variables between the low and high HR groups were compared using Mann-Whitney U test. The image-quality scores in the systolic and diastolic phases were compared using Wilcoxon's signed-rank test. To investigate the impact of the observer and cardiac phase on the RV-ECV measurements, we conducted a two-way repeated measure analysis of variance (ANOVA). The intra- and interobserver variabilities of ECV measurements were evaluated using intraclass correlation coefficient (ICC) values. The level of agreement was classified as follows: excellent, ICC >0.75; good, ICC =0.60–0.74; fair, ICC =0.40–0.59; and poor, ICC <0.40 (12).

Results

Study population

After excluding 16 patients with metal artifacts due to previous cardiac surgeries and 13 patients with poor image quality, 55 patients (HR >70, 28 patients; HR ≤70, 27 patients) were enrolled and analyzed in this study (*Figure 2*). Patient characteristics are shown in *Table 1*. The two HR groups showed no significant difference in age (68.5±14.1 *vs.* 67.5±15.2 years; P=0.89) and BMI (23.6±3.7 *vs.* 24.1±4.1; P=0.81), but showed significant differences in sex distribution (7 males and 20 females *vs.* 19 males and 9 females; P=0.0093).

Comparison of ECVs in the mid-diastolic and end-systolic phases

The ECVs of the septal regions during mid-diastole were significantly higher than those during end-systole (base: end-systole *vs.* mid-diastole, 26.6%±4.8% *vs.* 27.8%±5.1%, P=0.0011; mid-ventricle: end-systole *vs.* mid-diastole, 26.7%±4.4% *vs.* 28.2%±4.6%, P=0.0001) (*Table 2*). Other regions showed no significant differences (P=0.13–0.97) and similar ECV measurements in each group, except the LV anterior wall at the base-ventricular level (end-systole *vs.* mid-diastole, 24.7%±3.6% *vs.* 25.9%±4.8%, P=0.0181) and the LV posterior wall at the base-ventricular level (end-systole *vs.* mid-diastole, 27.2%±4.3% *vs.* 28.3%±4.5%, P=0.0061). The image-quality score in systole was significantly higher than that in diastole (systole *vs.* diastole: 3.6±0.5 *vs.* 3.2±0.7, P=0.0195).

Comparison of ECVs in the mid-diastolic and end-systolic phases in the high- and low-HR groups

The ECVs of the septal regions during mid-diastole

Table 2 Extracellular volume at each point between cardiac cycles

ECV location	Base			Mid		
	End-systole	Mid-diastole	P value	End-systole	Mid-diastole	P value
Septum (%)	26.6±4.8	27.8±5.1	0.0011	26.7±4.4	28.2±4.6	0.0001
Anterior (%)	24.7±3.6	25.9±4.8	0.0181	25.4±4.2	26.0±4.6	0.2204
Lateral (%)	27.5±4.0	27.3±3.9	0.7178	27.0±3.6	26.8±4.1	0.5874
Posterior (%)	27.2±4.3	28.3±4.5	0.0061	26.8±4.6	27.5±4.4	0.1316
RV anterior (%)	26.8±3.8	26.1±3.8	0.2264	26.5±4.3	26.5±4.8	0.9739
RV lateral (%)	26.2±4.0	25.9±4.6	0.3997	26.6±4.1	26.7±5.1	0.8333
RV posterior (%)	26.9±3.8	27.2±4.5	0.5207	27.8±3.7	28.0±5.0	0.5607

Values are expressed as mean ± standard deviation. ECV, extracellular volume; RV, right ventricle.

were significantly higher than those during end-systole in the high-HR group (base: end-systole *vs.* mid-diastole, 27.4%±4.9% *vs.* 28.5%±5.0%, P=0.0330; mid-ventricle: end-systole *vs.* mid-diastole, 27.3%±4.2% *vs.* 28.8%±5.0%, P=0.0133) and low-HR group (base: end-systole *vs.* mid-diastole, 25.9%±4.7% *vs.* 27.2%±5.1%, P=0.0160; mid-ventricle: end-systole *vs.* mid-diastole, 26.1%±4.6% *vs.* 27.6%±4.2%, P=0.0034) (Tables S1,S2). The other regions showed no significant differences in ECV measurements in both groups (P=0.059–0.97), except the LV anterior wall at the base-ventricular level in the high-HR group (end-systole *vs.* mid-diastole, 25.2%±4.3% *vs.* 26.6%±5.1%, P=0.0224) and the LV posterior wall at the base-ventricular level in the low-HR group (end-systole *vs.* mid-diastole, 26.8%±3.9% *vs.* 28.0%±4.6%, P=0.0491). The image-quality score in systole was significantly higher than that in diastole in the low-HR group (systole *vs.* diastole: 3.5±0.5 *vs.* 3.0±0.7, P=0.034) and high-HR group (systole *vs.* diastole: 3.6±0.5 *vs.* 3.0±0.7, P=0.049).

Inter- and intraobserver variabilities

Table 3 shows the intra- and interobserver variability of the ECV measurements at each ventricular level. The LV ECV measurements showed excellent agreement in both groups. However, the intra-and interobserver variabilities of RV ECV measurements at the end-systolic phase were higher than those at the mid-diastolic phase in almost all segments except the RV basal posterior wall {base: intraobserver, end-systole *vs.* mid-diastole, 0.817 [95% confidence interval (CI): 0.695–0.891] *vs.* 0.620 (95% CI: 0.366–0.773); interobserver, end-systole *vs.* mid-diastole, 0.602 (95% CI: 0.413–0.741) *vs.* 0.502 (95% CI: 0.289–0.668); mid-ventricle: intraobserver, end-systole *vs.* mid-diastole, 0.787 (95% CI: 0.645–0.873) *vs.* 0.327 (95% CI: –0.125–0.598); interobserver, end-systole *vs.* mid-diastole, 0.614 (95% CI: 0.430–0.750) *vs.* 0.380 (95% CI: 0.140–0.578)}. We conducted a repeated measures ANOVA to examine the influence of the cardiac phase and observer on the RV-ECV measurements. Our analysis revealed significant effects of the cardiac phase in the mid- and base-ventricular levels of the RV anterior wall, as well as the base ventricular level in the RV free wall, and the base ventricular level in the overall RV (P<0.0001–P=0.0184). However, no significant effects of cardiac phase were observed in the other areas (P=0.2632–0.3148). Furthermore, no significant effect of the observer was observed (P=0.1257–0.9622). It was observed that the cardiac phase affects the RV-ECV based on the observation location.

Discussion

The main findings of our study are as follows: (I) the ECVs of the septal regions at mid-diastole was significantly higher than that at end-systole, irrespective of HR; (II) the ECV values were similar in the other regions, including the RV, except the LV anterior and posterior wall at the base-ventricular level; (III) the image quality was better in end-systole than in mid-diastole, irrespective of HR; and (IV) reproducibility of RV-ECV measurements at the end-systolic phase was superior to that at the mid-diastolic phase.

Regardless of the HR, the ECV of the septum in the mid-diastolic phase was significantly higher than that in the end-systolic phase. This result was similar to those reported in previous studies using cardiac MRI (16). The difference in ECV between the end-systolic and mid-

Table 3 Inter- and intraobserver variability at each point

Location	Interobserver variability (95% CI)				Intraobserver variability (95% CI)			
	Base		Mid		Base		Mid	
	End-systole	Mid-diastole	End-systole	Mid-diastole	End-systole	Mid-diastole	End-systole	Mid-diastole
Septum	0.984 (0.960–0.994)	0.947 (0.872 –0.979)	0.931 (0.823–0.973)	0.937 (0.848–0.975)	0.989 (0.975–0.996)	0.980 (0.686–0.950)	0.984 (0.960–0.994)	0.959 (0.899–0.984)
Anterior	0.746 (0.432–0.894)	0.931 (0.837–0.972)	0.680 (0.341–0.861)	0.804 (0.569–0.917)	0.969 (0.923–0.988)	0.971 (0.928–0.988)	0.953 (0.883–0.981)	0.817 (0.546–0.927)
Lateral	0.544 (0.161–0.788)	0.791 (0.550–0.791)	0.733 (0.271–0.900)	0.595 (0.224–0.816)	0.954 (0.886–0.964)	0.874 (0.686–0.950)	0.866 (0.667–0.947)	0.844 (0.612–0.938)
Posterior	0.836 (0.636–0.931)	0.825 (0.284–0.994)	0.868 (0.694–0.946)	0.761 (0.492–0.898)	0.983 (0.957–0.993)	0.962 (0.957–0.993)	0.958 (0.896–0.983)	0.940 (0.851–0.976)
LV mean	0.868 (0.791–0.916)	0.899 (0.821–0.940)	0.832 (0.682–0.905)	0.798 (0.703–0.866)	0.981 (0.972–0.988)	0.961 (0.971–0.988)	0.952 (0.926–0.969)	0.907 (0.855–0.940)
RV anterior	0.600 (0.212–0.818)	0.430 (0.013–0.724)	0.566 (0.189–0.800)	0.161 (–0.265–0.546)	0.864 (0.663–0.946)	0.618 (0.051–0.848)	0.864 (0.663–0.946)	0.216 (–0.095–0.696)
RV lateral	0.625 (0.277–0.831)	0.401 (–0.094–0.704)	0.503 (0.087–0.769)	0.389 (–0.057–0.705)	0.812 (0.554–0.925)	0.556 (–0.103–0.823)	0.701 (0.258–0.881)	0.286 (–0.771–0.716)
RV posterior	0.600 (0.242–0.818)	0.691 (0.374–0.864)	0.634 (0.269–0.838)	0.385 (–0.053–0.700)	0.795 (0.492–0.918)	0.680 (0.206–0.872)	0.734 (0.341–0.894)	0.166 (–1.071–0.667)
RV mean	0.602 (0.413–0.741)	0.502 (0.289–0.668)	0.614 (0.430–0.750)	0.380 (0.140–0.578)	0.817 (0.695–0.891)	0.620 (0.366–0.773)	0.787 (0.645–0.873)	0.327 (–0.125–0.598)

CI, confidence interval; LV, left ventricle; RV, right ventricle.

diastole phases is expected to be mainly related to changes in myocardial blood volume (16). Although differences in reported numbers are related to differences in measurement techniques and study populations as well as the differences between *in vivo* and *ex vivo* studies, changes from diastole to systole in capillary volumes in the septum region have been shown to be larger than those in the lateral wall (decrease of 24.7% *vs.* 18.2%) (17,18). These differences in capillary volume during the cardiac cycle may have been reflected in the differences in ECV values in the septum and other regions. Moreover, the septum is less susceptible to motion artifacts and beam hardening; therefore, it is the most commonly used site for ECV measurement. However, this small but significant difference in ECV could influence the outcomes of repeated ECV measurements for the evaluation of treatment response and disease monitoring. Therefore, selection of the same cardiac phase for ECV measurements is crucial in these clinical settings. The other regions showed no significant differences in ECV between end-systole and mid-diastole, except for the anterior and posterior LV at the base-ventricular level. In these areas, potential for beam hardening effect exists due to adjacent chest wall structures and the liver, as reported in the literature (19,20). Moreover, ECV in low HR were slightly as higher than that of high HR in this study. The difference of ECV between low and high HR may be caused by disparity in the gender distribution. Women's ECV values were higher than that of men, as reported in a previous study (21). Our results of sub-analysis were significantly difference in gender between high and low HR groups. Therefore, our results were reflected to gender imbalance. In addition, a previous study had reported that the poor image quality of delayed myocardium enhancement affects the measurement of CT-ECV (22). In our results, the image quality score of end-systole was significantly higher than that of mid-diastole. The difference between the end-systolic ECV and mid-diastolic ECV may be influenced by the difference of image quality. Thus, these factors could influence the ECV values and should be taken into account.

In our study, the RV-ECV values in the mid-diastolic phase were not significantly different from those in the end-systolic phase. However, the intra- and interobserver variabilities of RV-ECV values at the mid-diastolic phase were lower than those at the end-systolic phase in almost all segments. The thinner RV wall and non-compacted trabeculae may have resulted in low reproducibility in the mid-diastolic phase (*Figure 3*). Myocardial fibrosis is categorized as replacement fibrosis expressed by late

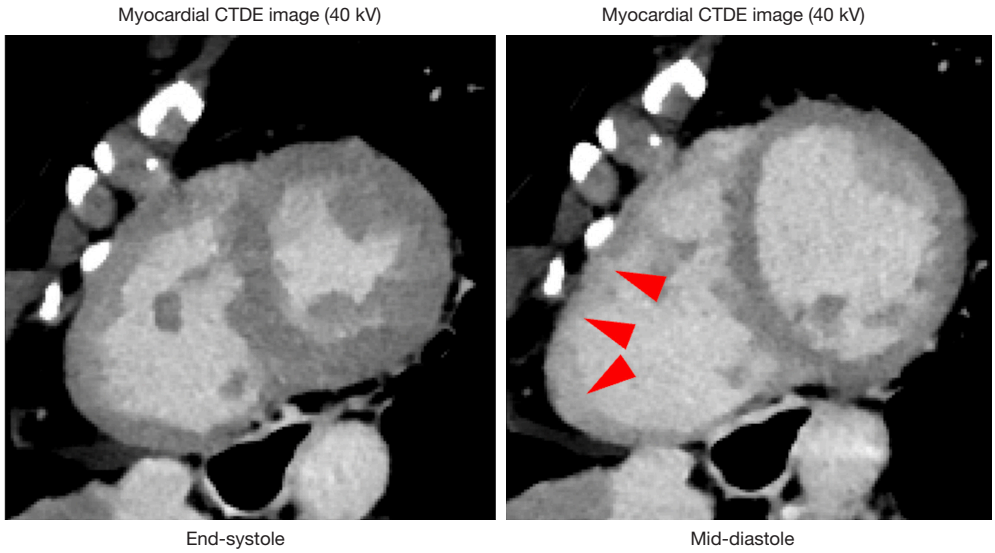

Figure 3 Reproducible ROI placement is difficult because of the thinner RV wall and non-compacted trabeculae in the mid-diastolic phase (arrowheads). CTDE, computed tomography delayed enhancement; ROI, region of interest; RV, right ventricle.

gadolinium enhancement and diffuse interstitial fibrosis expressed by ECV (23). The RV fibrosis induced by pulmonary hypertension is a potentially reversible form of reactive interstitial fibrosis, unlike the irreversible replacement fibrosis (24). Therefore, histological remodeling and reverse remodeling, which may be reflected by increased or decreased ECV values are important research targets in this field (25,26). Structural remodeling, e.g., a reduced RV volume, may be followed by histological remodeling. To our knowledge, this is the first study to prove that the end-systolic phase is suitable for repetitive RV-ECV measurements using DLCT, and the findings would greatly influence future investigations of pulmonary hypertension and congenital heart diseases.

Limitations

Our study had several limitations. First, this study was conducted at a single center with a relatively small cohort, potentially causing selection bias. Furthermore, we could not include a healthy control group for comparison because this investigation required the use of a contrast medium. Further studies with a large-scaled population are warranted to validate the results in the future. Second, our results were obtained with a detector-based dual-energy system from a single CT vendor; therefore, further evaluations should be performed with tube-based dual-energy CT systems (e.g., dual-source or fast kilovoltage-peak switching systems). Finally, additional radiation exposure was required to obtain CT-ECV results. Although further reduction of radiation exposure is desirable, it should be accomplished without sacrificing image quality.

Conclusions

Regardless of the HR, the ECV of the septal regions at mid-diastole was significantly higher than that at end-systole. The ECV in the other regions, including the RV, did not differ significantly in both groups, except for the LV anterior and posterior walls at the base-ventricular level. The image quality and reproducibility of ECV measurements in the end-systolic phase were superior to those in the mid-diastolic phase in the RV. Repetitive ECV measurements of the septum for evaluation of treatment response and disease monitoring should be performed in the same cardiac cycle. Additionally, ECV measurements of the RV should be preferably acquired at the end-systolic phase because of their high reproducibility.

Acknowledgments

We thank Junji Kishimoto, PhD (Kyushu University) for statistical analysis advice.
Funding: This work was supported by a research grant from KONICAMINOLTA; a grant named KAKENHI, from the Japan Society for the Promotion of Science (JSPS) (Nos.

JP20K16728 and JP23K07111); and the Konica Minolta Imaging Science Encouragement Award from Konica Minolta Science and Technology Foundation.

Footnote

Reporting Checklist: The authors have completed the STROBE reporting checklist. Available at https://qims.amegroups.com/article/view/10.21037/qims-23-1647/rc

Conflicts of Interest: All authors have completed the ICMJE uniform disclosure form (available at https://qims.amegroups.com/article/view/10.21037/qims-23-1647/coif). Y.Y. received research grants from JSPS (KAKENHI), KONICAMINOLTA, Inc., and Konica Minolta Science and Technology Foundation; and Honoraria for lectures from KONICAMINOLTA, Inc. T.H. received a research grant KAKENHI from JSPS. The other authors have no conflicts of interest to declare.

Ethical Statement: The authors are accountable for all aspects of the work in ensuring that questions related to the accuracy or integrity of any part of the work are appropriately investigated and resolved. The study was conducted in accordance with the Declaration of Helsinki (as revised in 2013). This retrospective observational study was approved by the Institutional Review Board of Kyushu University (No. 2023-72), and the requirement for informed consent was waived due to the retrospective nature of the study.

References

1. Sado DM, Flett AS, Banypersad SM, White SK, Maestrini V, Quarta G, Lachmann RH, Murphy E, Mehta A, Hughes DA, McKenna WJ, Taylor AM, Hausenloy DJ, Hawkins PN, Elliott PM, Moon JC. Cardiovascular magnetic resonance measurement of myocardial extracellular volume in health and disease. Heart 2012;98:1436-41.
2. Banypersad SM, Sado DM, Flett AS, Gibbs SD, Pinney JH, Maestrini V, Cox AT, Fontana M, Whelan CJ, Wechalekar AD, Hawkins PN, Moon JC. Quantification of myocardial extracellular volume fraction in systemic AL amyloidosis: an equilibrium contrast cardiovascular magnetic resonance study. Circ Cardiovasc Imaging 2013;6:34-9.
3. aus dem Siepen F, Buss SJ, Messroghli D, Andre F, Lossnitzer D, Seitz S, Keller M, Schnabel PA, Giannitsis E, Korosoglou G, Katus HA, Steen H. T1 mapping in dilated cardiomyopathy with cardiac magnetic resonance: quantification of diffuse myocardial fibrosis and comparison with endomyocardial biopsy. Eur Heart J Cardiovasc Imaging 2015;16:210-6.
4. Puntmann VO, Carr-White G, Jabbour A, Yu CY, Gebker R, Kelle S, Hinojar R, Doltra A, Varma N, Child N, Rogers T, Suna G, Arroyo Ucar E, Goodman B, Khan S, Dabir D, Herrmann E, Zeiher AM, Nagel E; International T1 Multicentre CMR Outcome Study. T1-Mapping and Outcome in Nonischemic Cardiomyopathy: All-Cause Mortality and Heart Failure. JACC Cardiovasc Imaging 2016;9:40-50.
5. Halliday BP, Gulati A, Ali A, Guha K, Newsome S, Arzanauskaite M, et al. Association Between Midwall Late Gadolinium Enhancement and Sudden Cardiac Death in Patients With Dilated Cardiomyopathy and Mild and Moderate Left Ventricular Systolic Dysfunction. Circulation 2017;135:2106-15.
6. Lee HJ, Im DJ, Youn JC, Chang S, Suh YJ, Hong YJ, Kim YJ, Hur J, Choi BW. Myocardial Extracellular Volume Fraction with Dual-Energy Equilibrium Contrast-enhanced Cardiac CT in Nonischemic Cardiomyopathy: A Prospective Comparison with Cardiac MR Imaging. Radiology 2016;280:49-57.
7. Wang R, Liu X, Schoepf UJ, van Assen M, Alimohamed I, Griffith LP, Luo T, Sun Z, Fan Z, Xu L. Extracellular volume quantitation using dual-energy CT in patients with heart failure: Comparison with 3T cardiac MR. Int J Cardiol 2018;268:236-40.
8. Ohta Y, Kitao S, Yunaga H, Watanabe T, Mukai-Yatagai N, Kishimoto J, Yamamoto K, Ogawa T. Quantitative evaluation of non-ischemic dilated cardiomyopathy by late iodine enhancement using rapid kV switching dual-energy computed tomography: A feasibility study. J Cardiovasc Comput Tomogr 2019;13:148-56.
9. Ohta Y, Kishimoto J, Kitao S, Yunaga H, Mukai-Yatagai N,

Fujii S, Yamamoto K, Fukuda T, Ogawa T. Investigation of myocardial extracellular volume fraction in heart failure patients using iodine map with rapid-kV switching dual-energy CT: Segmental comparison with MRI T1 mapping. J Cardiovasc Comput Tomogr 2020;14:349-55.
10. Qi RX, Shao J, Jiang JS, Ruan XW, Huang S, Zhang Q, Hu CH. Myocardial extracellular volume fraction quantitation using cardiac dual-energy CT with late iodine enhancement in patients with heart failure without coronary artery disease: A single-center prospective study. Eur J Radiol 2021;140:109743.
11. Qi RX, Jiang JS, Shao J, Zhang Q, Zheng KL, Xiao J, Huang S, Gong SC. Measurement of myocardial extracellular volume fraction in patients with heart failure with preserved ejection fraction using dual-energy computed tomography. Eur Radiol 2022;32:4253-63.
12. Yamasaki Y, Abe K, Kamitani T, Sagiyama K, Hida T, Hosokawa K, Matsuura Y, Hioki K, Nagao M, Yabuuchi H, Ishigami K. Right Ventricular Extracellular Volume with Dual-Layer Spectral Detector CT: Value in Chronic Thromboembolic Pulmonary Hypertension. Radiology 2021;298:589-96.
13. Kidoh M, Oda S, Takashio S, Tsujita K. Dynamic evaluation of myocardial extracellular volume fraction using dual-layer spectral detector computed tomography. Eur Heart J Case Rep 2020;4:1-2.
14. Herzog C, Arning-Erb M, Zangos S, Eichler K, Hammerstingl R, Dogan S, Ackermann H, Vogl TJ. Multi-detector row CT coronary angiography: influence of reconstruction technique and heart rate on image quality. Radiology 2006;238:75-86.
15. Oda S, Emoto T, Nakaura T, Kidoh M, Utsunomiya D, Funama Y, Nagayama Y, Takashio S, Ueda M, Yamashita T, Tsujita K, Ando Y, Yamashita Y. Myocardial Late Iodine Enhancement and Extracellular Volume Quantification with Dual-Layer Spectral Detector Dual-Energy Cardiac CT. Radiol Cardiothorac Imaging 2019;1:e180003.
16. Kawel N, Nacif M, Zavodni A, Jones J, Liu S, Sibley CT, Bluemke DA. T1 mapping of the myocardium: intra-individual assessment of the effect of field strength, cardiac cycle and variation by myocardial region. J Cardiovasc Magn Reson 2012;14:27.
17. Wu EX, Tang H, Wong KK, Wang J. Mapping cyclic change of regional myocardial blood volume using steady-state susceptibility effect of iron oxide nanoparticles. J Magn Reson Imaging 2004;19:50-8.
18. Wansapura J, Gottliebson W, Crotty E, Fleck R. Cyclic variation of T1 in the myocardium at 3 T. Magn Reson Imaging 2006;24:889-93.
19. Goo HW. Myocardial delayed-enhancement CT: initial experience in children and young adults. Pediatr Radiol 2017;47:1452-62.
20. Lee HJ, Im DJ, Youn JC, Chang S, Suh YJ, Hong YJ, Kim YJ, Hur J, Choi BW. Assessment of myocardial delayed enhancement with cardiac computed tomography in cardiomyopathies: a prospective comparison with delayed enhancement cardiac magnetic resonance imaging. Int J Cardiovasc Imaging 2017;33:577-84.
21. Rosmini S, Bulluck H, Captur G, Treibel TA, Abdel-Gadir A, Bhuva AN, Culotta V, Merghani A, Fontana M, Maestrini V, Herrey AS, Chow K, Thompson RB, Piechnik SK, Kellman P, Manisty C, Moon JC. Myocardial native T1 and extracellular volume with healthy ageing and gender. Eur Heart J Cardiovasc Imaging 2018;19:615-21.
22. Brodoefel H, Klumpp B, Reimann A, Ohmer M, Fenchel M, Schroeder S, Miller S, Claussen C, Kopp AF, Scheule AM. Late myocardial enhancement assessed by 64-MSCT in reperfused porcine myocardial infarction: diagnostic accuracy of low-dose CT protocols in comparison with magnetic resonance imaging. Eur Radiol 2007;17:475-83.
23. Senapati A, Malahfji M, Debs D, Yang EY, Nguyen DT, Graviss EA, Shah DJ. Regional Replacement and Diffuse Interstitial Fibrosis in Aortic Regurgitation: Prognostic Implications From Cardiac Magnetic Resonance. JACC Cardiovasc Imaging 2021;14:2170-82.
24. Andersen S, Nielsen-Kudsk JE, Vonk Noordegraaf A, de Man FS. Right Ventricular Fibrosis. Circulation 2019;139:269-85.
25. Kim PK, Hong YJ, Shim HS, Im DJ, Suh YJ, Lee KH, Hur J, Kim YJ, Choi BW, Lee HJ. Serial T1 mapping of right ventricle in pulmonary hypertension: comparison with histology in an animal study. J Cardiovasc Magn Reson 2021;23:64.
26. Schimmel K, Ichimura K, Reddy S, Haddad F, Spiekerkoetter E. Cardiac Fibrosis in the Pressure Overloaded Left and Right Ventricle as a Therapeutic Target. Front Cardiovasc Med 2022;9:886553.

Cite this article as: Nishigake D, Yamasaki Y, Hida T, Shirasaka T, Funatsu R, Kato T, Ishigami K. Influence of cardiac cycle on myocardial extracellular volume fraction measurements with dual-layer computed tomography. Quant Imaging Med Surg 2024;14(7):4714-4722. doi: 10.21037/qims-23-1647

